Journal of Organometallic Chemistry 696 (2011) 2728–2735

Contents lists available at ScienceDirect

Journal of Organometallic Chemistry

journal homepage: www.elsevier.com/locate/jorganchem

Cellular uptake, cytotoxicity, apoptosis, antioxidant activity and DNA binding of polypyridyl ruthenium(II) complexes

Yun-Jun Liu [a,*], Zhen-Hua Liang [a], Zheng-Zheng Li [a], Jun-Hua Yao [b], Hong-Liang Huang [c,*]

[a] School of Pharmacy, Guangdong Pharmaceutical University, Guangzhou 510006, PR China
[b] Instrumentation Analysis and Research Center, Sun Yat-Sen University, Guangzhou 510275, PR China
[c] School of Life Science and Biopharmaceutical, Guangdong Pharmaceutical University, Guangzhou 510006, PR China

ARTICLE INFO

Article history:
Received 10 February 2011
Received in revised form
14 April 2011
Accepted 19 April 2011

Keywords:
Ruthenium(II) complex
Cytotoxicity
Apoptosis
Cellular uptake
DNA binding

ABSTRACT

Ruthenium(II) polypyridyl complexes $[Ru(phen)_2(APIP)](ClO_4)_2$ **1** and $[Ru(phen)_2(HAPIP)](ClO_4)_2$ **2** have been synthesized and characterized. The DNA-binding behaviors were investigated by electronic absorption titration, luminescence spectra, viscosity measurements, thermal denaturation and photo-activated cleavage. The DNA-binding constants K_b for complexes **1** and **2** were determined to be 3.38 ($\pm$0.42) $\times$ 10^5 M^{-1} (s = 1.48) and 3.93 ($\pm$0.60) $\times$ 10^5 M^{-1} (s = 3.14), respectively. The studies on the photocleavage demonstrated that the effects of cleavage are concentration-dependent. The results showed that complexes **1** and **2** interact with CT-DNA by intercalative mode. The cytotoxicity of complexes **1** and **2** has been evaluated by MTT method. The apoptosis assay was carried out with acridine orange/ethidium bromide (AO/EB) staining methods. The cellular uptake showed that complexes can enter into the cytoplasm and accumulate in the nuclei. The antioxidant activity studies suggested that the ligands and complexes may be potential drugs to eliminate the radical.

1. Introduction

The intercalation of transition metal polypyridyl complexes into DNA has been a topic major bioinorganic interest in the past two decades and continues to receive much attention [1–3]. As an important target of anticancer drugs, DNA plays a central role in replication, transcription, and regulation of genes. The presence of metal-binding sites in DNA structure make different type of interactions possible such as intercalation between base pairs, minor groove binding, and major groove binding [4]. Complexes $[Ru(bpy)_2(dppz)]^{2+}$ [5] and $[Ru(bpy)_2(ppd)]^{2+}$ [6] bind to DNA with large affinities and may act as "molecular light switch". Which show no luminescence in aqueous buffer, but after bound to DNA by intercalation they can luminescence brightly. On the other hand, Ruthenium complexes are regarded as promising alternatives to platinum complexes and several ruthenium complexes have now been proposed as potential anticancer substances [7,8], some of them demonstrate remarkable anticancer activity [9–12]. Complex $[Ru(bpy)_2(dppn)]^{2+}$ can effectively inhibit the proliferation of MCF-7 cells with a low IC_{50} (3.3 $\pm$ 1.2 μM) [13]. $[Ru(phen)_2(paip)]^{2+}$ can effectively induce apoptosis of BEL-7402 cell line [14], and $[(\eta^6\text{-}C_6Me_6)RuCl(dppn)]^{2+}$, bearing an arene ligand, that facilitates diffusion through cell membrane and thereby enhances cellular uptake, shows a high cell uptake of 1054.7 ng Ru/mg protein on HT-29 (colon cancer) cells [15]. Our previous work showed that complexes formed by intercalative ligands containing amino-group possessed high antitumor activity [14,16]. In this article, two new ligands, APIP, and HAPIP bearing amino-group and their Ru(II) complexes $[Ru(phen)_2(APIP)](ClO_4)_2$ **1** $[Ru(phen)_2(HAPIP)](ClO_4)_2$ **2** (Scheme 1) have been synthesized and characterized by elemental analysis, ES-MS, and ^1H NMR. Their DNA-binding behaviors were investigated by absorption titration, viscosity measurements, thermal denaturation and photocleavage. The results showed that complexes **1** and **2** interact with CT-DNA by intercalative mode. The cytotoxicity of complexes **1** and **2** has been evaluated by MTT (MTT = (3-(4,5-dimethylthiazol-2-yl)-2,5-diphenyltetrazolium bromide)) assay. The apoptosis of BEL-7402 cells induced by Ru(II) complexes was also studied. The study on the cellular uptake with BEL-7402 cells was carried out and the results were observed under fluorescence microscopy. The antioxidant activity of these complexes was explored by hydroxyl radical (•OH) scavenging method in vitro.

Abbreviations: APIP, 2-(2′-aminophenyl)imidazo[4,5-*f*][1,10]phenanthroline; HAPIP, 2-(2′-hydroxyl-4-aminophenyl)imidazo[4,5-*f*][1,10]phenanthroline; CT-DNA, calf thymus DNA; MTT, 3-(4,5-dimethylthiazol-2-yl)-2,5-diphenyltetrazolium bromide; Phen, 1,10-phenanthroline; AO, Acridine orange; EB, ethidium bromide; DMSO, dimethylsulfoxide.

* Corresponding authors. Tel.: +86 20 39352122; fax: +86 20 39352128.
E-mail addresses: lyjche@163.com (Y.-J. Liu), honglianghuangcn@hotmail.com (H.-L. Huang).

0022-328X/$ – see front matter Crown Copyright © 2011 Published by Elsevier B.V. All rights reserved.
doi:10.1016/j.jorganchem.2011.04.020

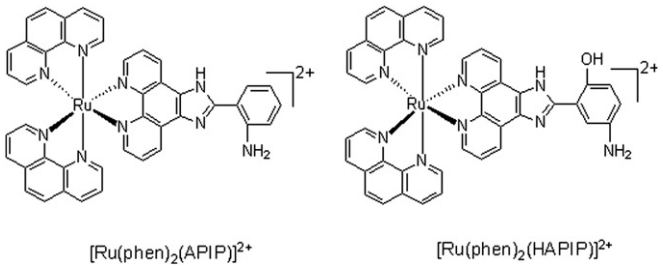

Scheme 1. The structure of complexes.

2. Experimental

2.1. Reagents and materials

Calf thymus DNA (CT-DNA) was obtained from the Sino-American Biotechnology Company. pBR 322 DNA was obtained from Shanghai Sangon Biological Engineering & Services Co., Ltd. Dimethylsulfoxide (DMSO) and RPMI 1640 were purchased from Sigma. Cell lines of BEL-7402 (hepatocellular), HepG-2 (hepatocellular) and MCF-7 (breast cancer) were purchased from American Type Culture Collection, agarose and ethidium bromide were obtained from Aldrich. $RuCl_3 \cdot xH_2O$ was purchased from Kunming Institution of Precious Metals. 1,10-Phenanthroline was obtained from Guangzhou Chemical Reagent Factory. Doubly distilled water was used to prepare buffers (5 mM Tris(hydroxymethylaminomethane)–HCl, 50 mM NaCl, pH = 7.2). A solution of CT-DNA in the buffer gave a ratio of UV absorbance at 260 and 280 nm of ca. 1.8–1.9:1, indicating that the DNA was sufficiently free of protein [17]. The DNA concentration per nucleotide was determined by absorption spectroscopy using the molar absorption coefficient (6600 M^{-1} cm^{-1}) at 260 nm [18].

2.2. Methods and instrumentation

Microanalysis (C, H, and N) was carried out with a Perkin–Elmer 240Q elemental analyzer. Fast atom bombardment (FAB) mass spectra were recorded on a VG ZAB-HS spectrometer in a 3-nitrobenzyl alcohol matrix. Electrospray mass spectra (ES-MS) were recorded on an LCQ system (Finnigan MAT, USA) using methanol as mobile phase. The spray voltage, tube lens offset, capillary voltage and capillary temperature were set at 4.50 kV, 30.00 V, 23.00 V and 200 °C, respectively, and the quoted *m/z* values are for the major peaks in the isotope distribution. ^{1}H NMR spectra were recorded on a Varian-500 spectrometer. All chemical shifts were given relative to tetramethylsilane (TMS). UV/vis spectra were recorded on a Shimadzu UV-3101PC spectrophotometer and emission spectra were recorded on a Shimadzu RF-4500 luminescence spectrometer at room temperature. The cellular uptake was observed under IX-50 inverted fluorescence microscopy (100×) with blue light as excitation.

2.3. Synthesis of ligands and complexes

2.3.1. 2-(2-Aminophenyl)imidazo [4,5-f][1,10]phenanthroline (APIP)

A mixture of 2-(2-nitrophenyl)imidazo [4,5-*f*][1,10]phenanthroline (0.171 g, 0.5 mmol) (NPIP) [19] was completely dissolved in ethanol (50 cm^3) with stirring for 1 h. Then the Pd/C (0.20 g, 10% Pd) and $NH_2NH_2 \cdot H_2O$ (8 cm^3) were added in the above solution and refluxed for 6 h. The hot solution was filtered and evaporated to remove the solvent under reduced pressure. The red compound obtained was washed with cool ethanol and dried at 50 °C in vacuo. Yield: 73%. Anal. Calcd. for $C_{19}H_{13}N_5$: C, 73.30; H, 4.21; N, 22.49; Found: C, 73.16; H, 4.13; N, 22.38%. FAB-MS: $m/z = 312$ $[M+1]^+$. ^{1}H NMR (500 MHz, DMSO-d_6): 9.05 (d, 2H, J = 8.0 Hz), 8.98(d, 2H, J = 8.2 Hz), 8.02–8.05 (m, 2H), 7.83 (d, 1H, J = 8.0 Hz), 7.18–7.35 (m, 1H), 6.92 (d, 1H, J = 8.0 Hz), 6.74(t, 1H, J = 7.6 Hz), 3.36 (s, 2H, H_{NH2}).

2.3.2. 2-(2-Hydroxyl-5-aminophenyl)imidazo [4,5-f][1,10] phenanthroline (HAPIP)

This compound was prepared in a manner identical to that described for APIP, with 2-(2-hydroxyl-5-nitrophenyl)imidazo [4,5-*f*][1,10]phenanthroline [20] in place of 2-(2-nitrophenyl)imidazo [4,5-*f*][1,10]phenanthroline. Yield: 73%. Anal. Calcd. for $C_{19}H_{13}N_5O$: C, 69.72; H, 4.00; N, 21.39; Found: C, 69.60; H, 4.13; N, 21.52%. FAB-MS: $m/z = 328$ $[M+1]^+$. ^{1}H NMR (500 MHz, DMSO-d_6): 9.06 (d, 2H, J = 8.2 Hz), 8.98(d, 2H, J = 7.5 Hz), 7.87 (dd, 2H, J = 8.0 Hz), 7.43 (d, 1H, J = 8.0 Hz), 6.84 (d, 1H, J = 8.6 Hz), 6.73–6.75 (m, 1H), 3.39 (s, 2H, H_{NH2}).

2.3.3. $[Ru(phen)_2(APIP)](ClO_4)_2 \cdot 2H_2O$ (**1**)

$[Ru(phen)_2(NPIP)](ClO_4)_2$ (0.509 g, 0.5 mmol) [19] was completely dissolved in acetronitrile. Then the ethanol of 50 cm^3, Pd/C (0.20 g, 10% Pd) and $NH_2NH_2 \cdot H_2O$ (8 cm^3) were added in the above solution and refluxed under argon for 8 h to give a clear red solution. Upon cooling, a red precipitate was obtained by dropwise addition of saturated aqueous $NaClO_4$ solution. The crude product was purified by column chromatography on a neutral alumina with a mixture of CH_3CN/toluene (3:1, v/v) as eluent. The main red band was collected. The solvent was removed under reduced pressure and a red powder was obtained. Yield: 70%. Anal. Calcd. for $C_{43}H_{29}N_9Cl_2O_8Ru \cdot 2H_2O$: C, 51.25; H, 3.30; N, 12.51; Found: C, 51.72; H, 3.59; N, 12.94%. ES-MS [CH_3CN, *m/z*]: 771.5 ($[M - 2ClO_4 - H]^+$), 386.4 ($[M - 2ClO_4]^{2+}$). ^{1}H NMR (500 MHz, DMSO-d_6): δ 8.78 (d, 4H, J = 8.2 Hz), 8.40 (s, 4H), 8.17 (d, 2H, J = 8.2 Hz), 8.12 (d, 4H, J = 8.0 Hz), 8.08 (d, 2H, J = 8.0 Hz), 7.98 (d, 2H, J = 8.2 Hz), 7.75–7.78 (m, 5H), 7.20 (t, 1H, J = 7.6), 6.91 (d, 1H, J = 8.0 Hz), 6.74 (t, 1H, J = 7.8 Hz), 3.37 (s, 2H, H_{NH2}).

2.3.4. $[Ru(phen)_2(HAPIP)](ClO_4)_2 \cdot 2H_2O$ (**2**)

A mixture of *cis*-$[Ru(phen)_2Cl_2] \cdot 2H_2O$ [21] (0.280 g, 0.5 mmol) and HAPIP (0.164 g, 0.5 mmol) in ethanol (30 cm^3) was refluxed under argon for 8 h to give a clear red solution. Upon cooling, a red precipitate was obtained by dropwise addition of saturated aqueous $NaClO_4$ solution. The crude product was purified by column chromatography on a neutral alumina with a mixture of CH_3CN–toluene (3:1, v/v) as eluant. The main red band was collected. The solvent was removed under reduced pressure and a red powder was obtained. Yield: 72%. Anal. Calcd. for $C_{43}H_{29}N_9Cl_2O_9Ru \cdot 2H_2O$: C, 50.45; H, 3.25; N, 12.31; Found: C, 50.64; H, 3.63; N, 12.78%. ES-MS [CH_3CN, *m/z*]: 788.3 ($[M - 2ClO_4 - H]^+$), 394.8 ($[M - 2ClO_4]^{2+}$). ^{1}H NMR (500 MHz, DMSO-d_6): δ 8.82 (d, 2H, J = 8.0 Hz), 8.76 (d, 4H, J = 8.0 Hz), 8.67 (d, 2H, J = 8.5 Hz), 8.47 (d, 1H, J = 8.0 Hz), 8.38 (s, 4H), 8.10 (t, 4H, J = 7.6 Hz), 7.74–7.78 (m, 6H), 7.60 (dd, 2H, J = 7.8 Hz), 3.35 (s, 2H).

Caution: Perchlorate salts of metal compounds with organic ligands are potentially explosive, and only small amounts of the material should be prepared and handled with great care.

2.4. DNA-binding assays

The DNA-binding and photoactivated cleavage experiments were performed at room temperature. Buffer A (5 mM Tris, 50 mM NaCl, pH 7.0) was used for absorption titration, luminescence titration and viscosity measurements. Buffer B (50 mM Tris–HCl, 18 mM NaCl, pH 7.2) was used for DNA photocleavage experiments. Buffer C (1.5 mM Na_2HPO_4, 0.5 mM NaH_2PO_4, 0.25 mM Na_2EDTA, pH 7.0) was used for thermal DNA denaturation experiments. Buffer

D (0.9% of physiological saline) was used for retardation assay of pGL 3 plasmid DNA.

The absorption titrations of the complex in buffer were performed using a fixed concentration (20 μM) for complex to which increments of the DNA stock solution were added. Ru/DNA solutions were allowed to incubate for 5 min before the absorption spectra were recorded. The intrinsic binding constants *K*, based on the absorption titration, were measured by monitoring the changes of absorption in the metal-to-ligand charge transition (MLCT) band with increasing concentration of DNA using the following equation [22].

$$\left(\varepsilon_a - \varepsilon_f\right)/\left(\varepsilon_b - \varepsilon_f\right) = \left(b - \left(b^2 - 2K^2C_t[\mathrm{DNA}]/s\right)\right)^{1/2}/2KC_t \quad (1a)$$

$$b = 1 + KC_t + K[\mathrm{DNA}]/2s \quad (1b)$$

where [DNA] is the concentration of CT-DNA in base pairs, the apparent absorption coefficients ε_a, ε_f and ε_b correspond to A_{obsed}/[Ru], the extinction coefficient for the free ruthenium complex, and the extinction coefficient for the ruthenium complex in fully bound form, respectively. *K* is the equilibrium binding constant in M^{-1}, C_t is the total metal complex concentration in nucleotides and *s* is the binding size.

Thermal denaturation studies were carried out with a Perkin–Elmer Lambda 35 spectrophotometer equipped with a Peltier temperature-controlling programmer (±0.1 °C). The melting temperature (T_m) was taken as the mid-point of the hyperchromic transition. The melting curves were obtained by measuring the absorbance at 260 nm for solutions of CT-DNA (80 μM) in the absence and presence of the Ru(II) complex (30 μM) as a function of the temperature. The temperature was scanned from 50 to 90 °C at a speed of 1 °C min^{-1}. The data were presented as $(A - A_0)/(A_f - A_0)$ versus temperature, where *A*, A_0, and A_f are the observed, the initial, and the final absorbance at 260 nm, respectively.

Viscosity measurements were carried out using an Ubbelodhe viscometer maintained at a constant temperature at 25.0 (±0.1) °C in a thermostatic bath. DNA samples approximately 200 base pairs in average length were prepared by sonicating in order to minimize complexities arising from DNA flexibility [23]. Flow time was measured with a digital stopwatch, and each sample was measured three times, and an average flow time was calculated. Relative viscosities for DNA in the presence and absence of complexes were calculated from the relation $\eta = (t - t^0)/t^0$, where *t* is the observed flow time of the DNA-containing solution and t^0 is the flow time of buffer alone [5,24]. Data were presented as $(\eta/\eta_0)^{1/3}$ versus binding ratio [25], where η is the viscosity of DNA in the presence of complexes and η_0 is the viscosity of DNA alone.

For the gel electrophoresis experiment, supercoiled pBR 322 DNA (0.1 μg) was treated with the Ru(II) complexes in buffer B, and the solution was then irradiated at room temperature with a UV lamp (365 nm, 10 W). The samples were analyzed by electrophoresis for 1.5 h at 80 V on a 1.0% agarose gel in TBE (89 mM Tris-borate acid, 2 mM EDTA, pH = 8.3). The gel was stained with 1 μg/ml ethidium bromide and photographed on an Alpha Innotech IS-5500 fluorescence chemiluminescence and visible imaging system.

2.5. Cytotoxicity assay

Cytotoxicity of complexes **1** and **2** was evaluated by using standard MTT (3-(4,5-dimethylthiazole)-2,5-diphenyltetraazolium bromide) assay [26]. Cells were placed in 96-well microassay culture plates (8×10^3 cells per well) and grown overnight at 37 °C in a 5% CO_2 incubator. Compounds tested were then added to the wells to achieve final concentrations ranging from 6.25 μM to 400 μM. Control wells were prepared by addition of culture medium (100 μL). Wells containing culture medium without cells were used as blanks. The plates were incubated at 37 °C in a 5% CO_2 incubator for 48 h. Upon completion of the incubation, stock MTT dye solution (20 μL, 5 mg mL^{-1}) was added to each well. After 4h incubation, buffer (100 μL) containing *N*,*N*-dimethylformamide (50%) and sodium dodecyl sulfate (20%) was added to solubilize the MTT formazan. The culture medium and cisplatin act as the negative and positive control, respectively. The optical density of each well was then measured on a microplate spectrophotometer at a wavelength of 490 nm. The IC_{50} values were determined by plotting the percentage viability versus concentration on a logarithmic graph and reading off the concentration at which 50% of cells remain viable relative to the control. Each experiment was repeated at least three times to get the mean values. Three different tumor cell lines (BEL-7402, HepG-2 and MCF-7) were the subjects of this study.

2.6. Apoptosis study

Apoptosis studies were performed with a staining method utilizing acridine orange (AO) and ethidium bromide (EB) [27]. According to the difference in membrane integrity between necrotic and apoptosis. AO can pass through cell membrane of living or early apoptotic cells, while staining by EB indicates loss of membrane integrityt. Under fluorescence microscope, live cells appear green. Necrotic cells stain red but have a nuclear morphology resembling that of viable cells. Apoptosis cells appear green, and morphological changes such as cell blebbing and formation of apoptotic bodies will be observed.

A monolayer of BEL-7402 cells was incubated in the absence or presence of complex **2** at concentration of 50 μM at 37 °C and 5% CO_2 for 48 h. After 48 h, each cell culture was stained with AO/EB solution (100 μg ml^{-1} AO, 100 μg ml^{-1} EB). Samples were observed under a fluorescence microscope.

2.7. Cellular uptake

Cells were placed in 24-well microassay culture plates (4×10^4 cells per well) and grown overnight at 37 °C in a 5% CO_2 incubator. Complexes tested were then added to the wells. The plates were incubated at 37 °C in a 5% CO_2 incubator for 48 h. Upon completion of the incubation, the wells were washed three times with phosphate buffered saline (PBS), after removing the culture medium, the cells were visualized by fluorescent microscopy.

2.8. Scavenger measurements of hydroxyl radical (•OH)

Scavenging measurements on hydroxyl radical (•OH) were carried out in aqueous media. The hydroxyl radical (•OH) was generated by the Fenton system [28]. The solution of the tested complexes was prepared with DMF (*N*,*N*-dimethylformamide). The assay mixture (5 mL) contained following reagents: safranin (28.5 μM), EDTA-Fe(II) (100 μM), H_2O_2 (44.0 μM), the tested compounds (0.5–3.5 μM) and a phosphate buffer (67 mM, pH = 7.4). The assay mixtures were incubated at 37 °C for 30 min in a water bath, after which, the absorbance was measured at 520 nm. All the tests were run in triplicate and expressed as the mean. A_i was the absorbance in the presence of the tested compound; A_0 was the absorbance in the absence of tested compounds; A_c was the absorbance in the absence of tested compound, EDTA-Fe(II), H_2O_2. The suppression ratio (η_a) was calculated on the basis of $(A_i - A_0)/(A_c - A_0) \times 100\%$.

3. Results and discussion

3.1. Synthesis and characterization

Complexes **1** and **2** were prepared by heating of ligands with *cis*-$[Ru(phen)_2Cl_2]$. The ligands, APIP and HAPIP, were synthesized with a method similar to that described by Steck and Day [29]. The structures of the ligands and their complexes were confirmed by elemental analysis, FAB-MS, ES-MS, and ^1H NMR. The chemical shifts of protons on the nitrogen atoms of imidazole ring were not observed, probably because the protons are very active and easy to be exchanged between the two nitrogens of the imidazole ring in solution. In the ES-MS spectra for the complexes **1** and **2**, as expected, the intense signals for $[M - 2ClO_4 - H]^+$ and $[M - 2ClO_4]^{2+}$ were observed, the obtained molecular weights were consistent with the expected values.

3.2. Absorption spectral studies

Upon increasing amounts of calf thymus DNA (CT-DNA) to complexes **1** and **2** in buffer A, the changes in absorbance at MLCT transition bands (455 nm for **1** and 460 nm for **2**) are observed. The observed hypochromisms are 23.07 and 28.95% with red shifts of 2 and 1 nm for **1** and **2**, respectively (Fig. 1). Therefore these spectral characteristics suggest that these complexes interact with DNA most likely through a mode that involves a stacking interaction between the aromatic chromophore and the base pairs of DNA. The intrinsic constants K_b were determined by monitoring the changes of absorbance in the MLCT band with increasing concentration of CT-DNA. The values of K_b are 3.38 ($\pm$0.42) $\times$ 10^5 M^{-1} ($s = 1.48$) and 3.93 ($\pm$0.60) $\times$ 10^5 M^{-1} ($s = 3.14$) M^{-1} for **1** and **2**, respectively. These are of the same order as that reported for $[Ru(bpy)_2(PIP)]^{2+}$ ($4.7 \pm 0.20 \times 10^5$ M^{-1}) [30] and $[Ru(phen)_2(HPIP)]^{2+}$ (9.10×10^5 M^{-1}) [31], $[Ru(phen)_2(PPIP)]^{2+}$ ($1.10 \pm 0.30 \times 10^5$ M^{-1}) [32], but is smaller than those of $[Ru(phen)_2(dppz)]^{2+}$ (5.1×10^6 M^{-1}) [33] and $[Ru(pdto)(dppz)]^{2+}$ ($3.0 \pm 0.01 \times 10^6$ M^{-1}) [34].

3.3. Viscosity measurements

In order to clarify the binding mode of ruthenium(II) complexes **1** and **2** with DNA, viscosity of DNA solutions containing varying amount of added complexes were measured. A classical intercalation of a ligand into DNA is known to cause a significant increase in the viscosity of a DNA solution due to an increase in the separation of the base pairs at the intercalation site and, hence, an increase in the overall DNA molecular length [35]. The effects of complexes **1**, **2** on the viscosity of rod-like DNA are shown in Fig. 2. Upon increasing the amounts of complexes **1** and **2**, the relative viscosity of CT-DNA solution increases steadily. The increased degree of viscosity, which may depend on its affinity to DNA, follows the order **2** > **1**. These results suggest that complexes **1** and **2** can bind to CT-DNA through intercalation mode.

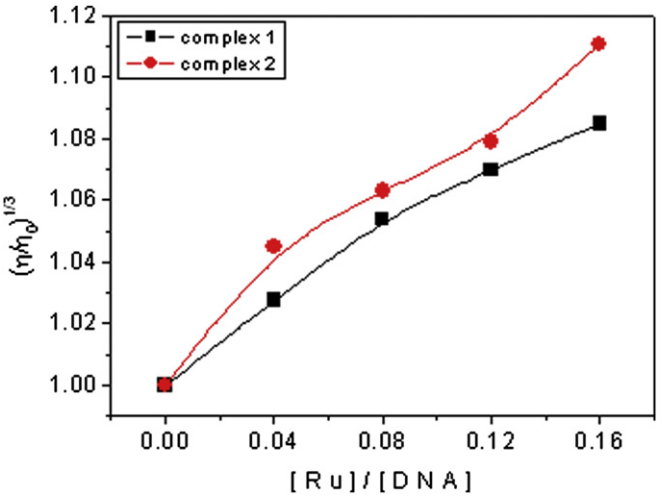

Fig. 2. Effect of increasing amounts of complexes **1** (■) and **2** (●) on the relative viscosity of CT-DNA at 25 ($\pm$0.1) °C. [DNA] = 0.25 mM.

3.4. Thermal denaturation

It is well known that complexes which intercalate between the base pairs of DNA can stabilize the duplex structure. The increase in absorbance at 260 nm was recorded from 40 to 90 °C, and T_m was then determined from the denaturation curve. The thermal denaturation experiments carried out on DNA in the absence of complexes revealed that the T_m for the duplex is 60.6 $\pm$ 0.5 °C under our experimental conditions. As shown in Fig. 3. The observed change of melting temperatures (ΔT_m) in the presence of complexes **1** and **2** are 7.8 and 11.3 °C, respectively. The large change in T_m suggests the binding affinities of both complexes with DNA are very strong. The binding constants of complexes **1** and **2** to CT-DNA at T_m were determined by McGee's equation [22].

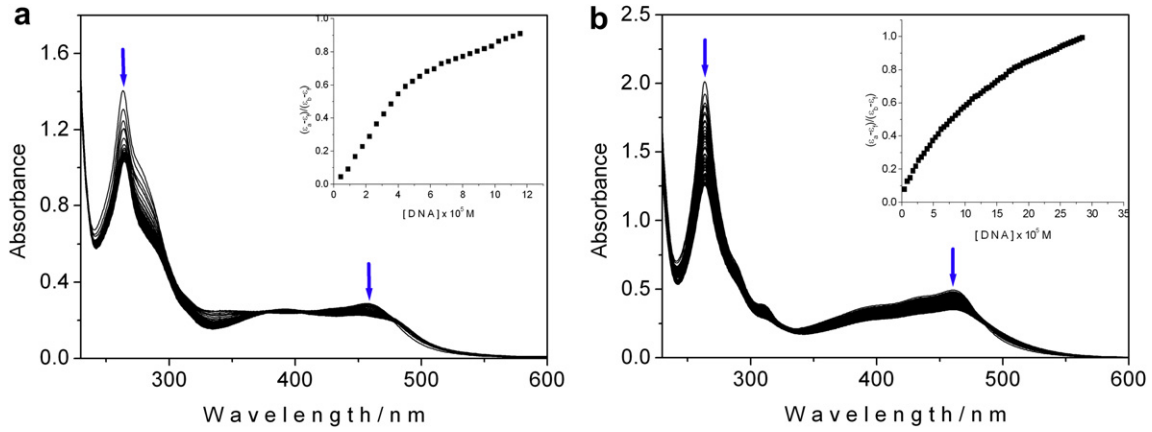

Fig. 1. Absorption spectra of complexes **1** (a) and **2** (b) in Tris–HCl buffer upon addition of increasing concentrations of CT-DNA. [Ru] = 20 μM. Arrow shows the absorbance change upon the increase of DNA concentration. Plots of $(\varepsilon_a - \varepsilon_f)/(\varepsilon_b - \varepsilon_f)$ versus [DNA] for the titration of DNA with Ru(II) complexes.

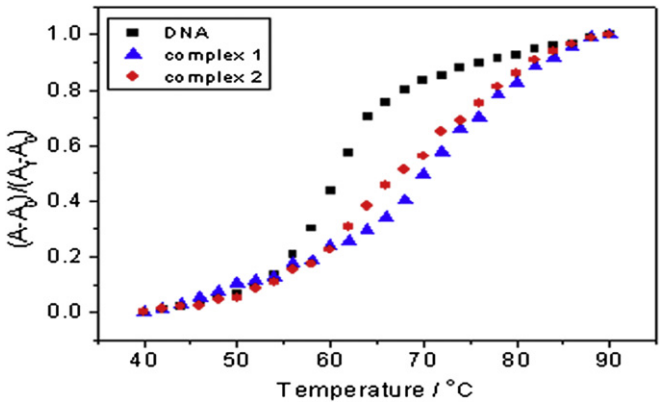

Fig. 3. Thermal denaturation of CT-DNA in the absence (■) and presence of complexes **1** (●) and **2** (▲). [Ru] = 30 μM, [DNA] = 80 μM.

$$\frac{1}{T_m^0} - \frac{1}{T_m} = \frac{R}{\Delta H_m}\ln(1 + KL)^{\frac{1}{n}} \quad (2)$$

where T_m^0 and T_m are the melting temperature of CT-DNA alone and in the presence of complex, respectively. ΔH_m is the enthalpy of DNA melting (per bp), R is the gas constant, K is the DNA-binding constant at T_m, L is the concentration of free Ru(II) complex, and n is the binding site size.

The value of $\Delta H_m = 6.9$ kcal mol^{-1} was determined by different scanning calorimetry [36]. On the basis of the absorption spectra titration experiment and the neighbor-exclusion principle, the values of n for both complexes were assumed to be 2.0 base pairs. The binding constants K for complex **1** and **2** at T_m were calculated to be 2.90×10^4 and 6.15×10^4 M^{-1}, respectively. According to the van't Hoffs equations (2)–(4) [37]

$$\ln\left(\frac{K_2}{K_1}\right) = \frac{\Delta H^0}{R}\left(\frac{1}{T_1} - \frac{1}{T_2}\right) \quad (3)$$

$$\Delta G_T^0 = -\mathrm{RT}\ln K \quad (4)$$

$$\Delta G_T^0 = \Delta H - T\Delta S^0 \quad (5)$$

where K_1 and K_2 are the DNA-binding constants of the complexes at the temperature of T_1 and T_2, respectively. ΔH^0, ΔG_T^0 and ΔS^0 are the changes of standard enthalpy, standard free energy and standard entropy of binding of the complex to CT-DNA. The values of ΔG_T^0, ΔH^0, and ΔS^0 were −31.54 kJ mol^{-1}, −47.86 kJ mol^{-1} and −54.76 J mol^{-1} K^{-1} for complex **1**, and −31.92 kJ mol^{-1}, −33.79 kJ mol^{-1} and −6.27 J mol^{-1} K^{-1} for complex **2**.

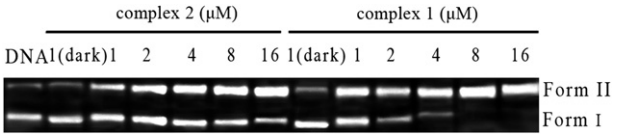

Fig. 5. Photoactivated cleavage of pBR 322 DNA in the presence of different concentrations of Ru(II) complexes after irradiation at 365 nm for 30 min.

3.5. Luminescence spectra studies

Complexes **1** and **2** can luminescence in Tris buffer at ambient temperature, with a maximum appearing at 590 and 592 nm for **1** and **2**, respectively. The luminescence spectra and the change of emission intensity are shown in Fig. 4. When the ratio of [DNA]/[Ru] reached 12.46 for **1** and 13.35 for **2**, the emission intensities of complexes **1** and **2** increase to 1.13 and 1.75 times of the original intensities, respectively. This implies that these complexes can interact with DNA and be protected by the hydrophobic environment inside the DNA helix efficiently.

3.6. Agarose gel electrophoresis

There is a particular ongoing interest in DNA cleavage reactions photoactivated by metal complexes [38,39]. The cleavage reaction on plasmid DNA can be monitored by agarose gel electrophoresis. When circular plasmid DNA is subjected to electrophoresis, relatively fast migration will be observed for the intact supercoiled form (Form I); if scission occurs on one strand (nicked), the supercoiled form will relax to generate a slower-moving open circular form (Form II) [40]. As seen in Fig. 5, control photoreaction with DNA alone or incubation with the ruthenium complexes in darkness results in little DNA cleavage. With increasing concentrations of the Ru(II) complexes, the amount of Form I was gradually diminished, whereas Form II increased. Comparing the cleaving effect of complexes **1** and **2**, complex **1** exhibits more effective DNA cleavage activity than complex **2**, which is not consistent with the DNA-binding affinity of two Ru(II) complexes.

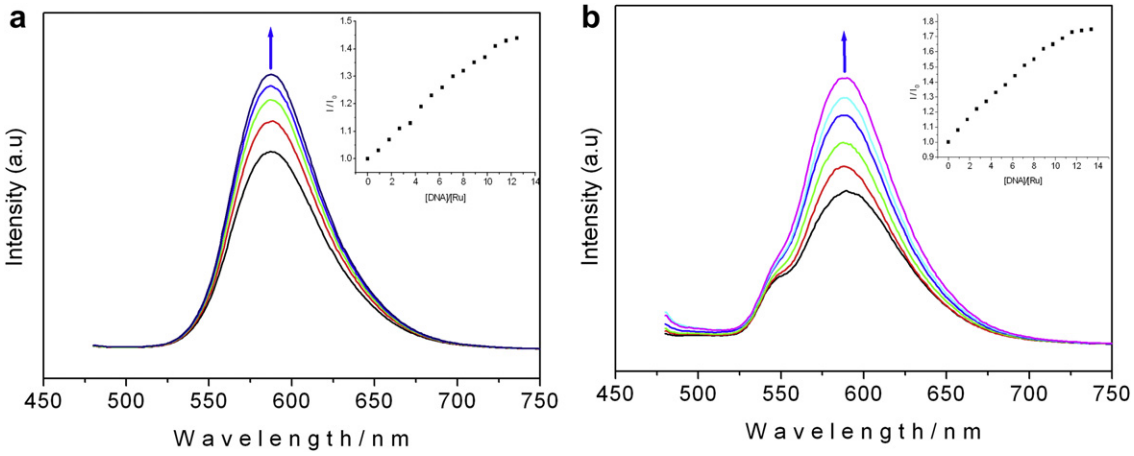

Fig. 4. Emission spectra of complexes a) **1** and b) **2** in Tris–HCl buffer in the absence and presence of CT-DNA. Arrow shows the intensity change upon increasing DNA concentrations.

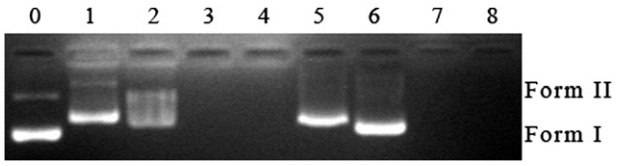

Fig. 6. Agarose gel electrophoresis retardation of pGL 3 plasmid DNA in the presence different concentrations of complexes **1** and **2**. Lane 0 (DNA alone); **1**: (1) 1 mM; (2) 2 mM; (3) 4 mM; (4) 6 mM. **2**: (5) 1 mM; (6) 2 mM; (7) 4 mM; (8) 6 mM [DNA] = 0.5 μg.

Table 1
The IC_{50} values for APIP, HAPIP, complexes **1** and **2** against selected cell lines.

Compound	IC50 (μM)		
	BEL-7402	HepG-2	MCF-7
PHEN	26.57 ± 2.78	–	–
APIP	18.47 ± 3.26	42.98 ± 2.54	21.14 ± 3.13
HAPIP	32.47 ± 2.77	45.35 ± 3.25	33.13 ± 3.42
1	43.07 ± 2.73	35.17 ± 2.78	44.35 ± 3.12
2	179.82 ± 5.66	146.25 ± 6.43	235.14 ± 6.47
Cisplatin	19.78 ± 2.55	25.48 ± 3.15	12.24 ± 2.55

3.7. Retardation of pGL 3 plasmid DNA

DNA condensation is prerequisite for efficient gene delivery using nonviral vectors. It is well known that polyamine can effectively condense DNA [41,42]. In recent years, the small molecules to condense DNA have been paid great attention. Complex $[Ru(bpy)_2(PIPSH)]^{2+}$ [43] can condense DNA at a concentration of 80 μM. And complex $Cu_2(egtb)(ClO_4)_2(H_2O)_2]^{2+}$ [44] can effectively and rapidly condense free DNA. The abilities of complexes **1** and **2** to condense pGL 3 DNA were assessed by gel retardation assay. Fig. 6 showed when the concentrations of complexes **1** and **2** are 1 and 2 mM, complexes **1** and **2** cannot condense the DNA. At the high concentrations of 4 and 6 mM, complexes **1** and **2** can effectively condense DNA.

3.8. Cytotoxicity assay in vitro

The cytotoxicity of $RuCl_3$, PHEN, APIP, HAPIP and complexes **1** and **2** was evaluated by MTT with three cell lines: BEL-7402, hepG-2 and MCF-7. The concentrations of these compounds ranged from 6.25 μM to 400 μM. The IC50 values obtained of these compounds against the selected four tumor cell lines are listed in Table 1. The resulting concentration-effect curves obtained with continuous exposure for 48 h are depicted in Fig. 7. The results showed that $RuCl_3$ has no cytotoxicity against selected cell lines. The IC50 values for complexes **1** and **2** ranged from 35.17 to 235.14 μM, suggesting that complexes **1** and **2** exhibited antitumor activity against the selected cell lines in different degree. Comparing the cytotoxicity of complexes **1** and **2**, complex **1** displayed higher cytotoxicity than complex **2**, but these complexes all exhibit relatively lower cytotoxicity in vitro than cisplatin. Furthermore, we also found that the coordination of the APIP and HAPIP to the Ru(II) metal center to form complexes **1** and **2**, the antitumor activity of two ligands was obviously weakened. And the cytotoxicity of phen located between APIP and HAPIP. Fig. 7 was the antiproliferative activity for ligands, complexes **1** and **2** against the selected cell lines, with the increasing concentration of these compounds, the proliferation of tumor cells was effectively inhibited.

3.9. Apoptosis induced by Ru(II) complexes

Apoptosis induced by compounds is one of the considerations in drug development. The apoptotic cells usually show apoptotic features such as nuclear shrinkage and chromatin condensation. Apoptosis assay was carried out with a staining method using acridine orange (AO) and ethidium bromide (EB). The AO/EB staining is sensitive to DNA and was used to assess the changes in nuclear morphology. Apoptotic and necrotic cells can be distinguished from one another using fluorescence microscopy. In the presence of complex **2**, the living cells were stained bright green in spots (Fig. 8A). After treatment of BEL-7402 cell line with complex **2** for a period of 48 h, green apoptotic cells containing apoptotic bodies stained by acridine orange, as well as red necrotic cells stained by ethidium bromide, were also found (Fig. 8B). Similar results for complex **1** were also observed.

3.10. Celluar uptake study

The spectroscopic data and viscosity measurements showed that complexes **1** and **2** can intercalate between the base pairs of CT-DNA. This prompted us to consider whether these complexes can cross the cell membrane and enter into the cytoplasm and accumulate in the nuclei. In order to prove our hypothesis, the cellular uptake with BEL-7402 cells was carried out. Complexes **1** (25 μM) and **2** (50 μM) were added to the well (4×10^4 cells per well). After treatment for 48 h, the cells were observed under fluorescent microscopy. As shown in Fig. 9, for cells treated with complexes **1** and **2**, the bright red fluorescent spots in the images were observed, whereas no any red fluorescent spots was observed in the control (data not presented). These results indicated that complex **1** and **2** can enter into the cytoplasm and accumulate in the nuclei.

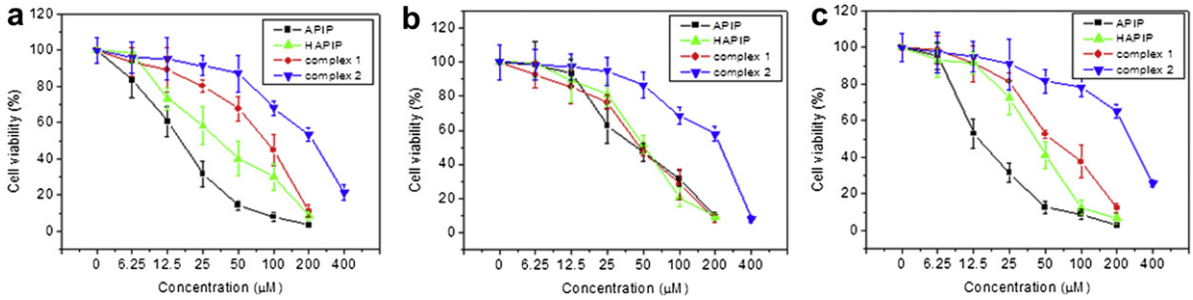

Fig. 7. Cell viability of APIP, HAPIP, complexes **1** and **2** on tumor BEL-7402 (a), HepG-2 (b) and MCF-7 (c) cell proliferation in vitro. Each data point is the mean ± standard error obtained from at least three independent experiments.

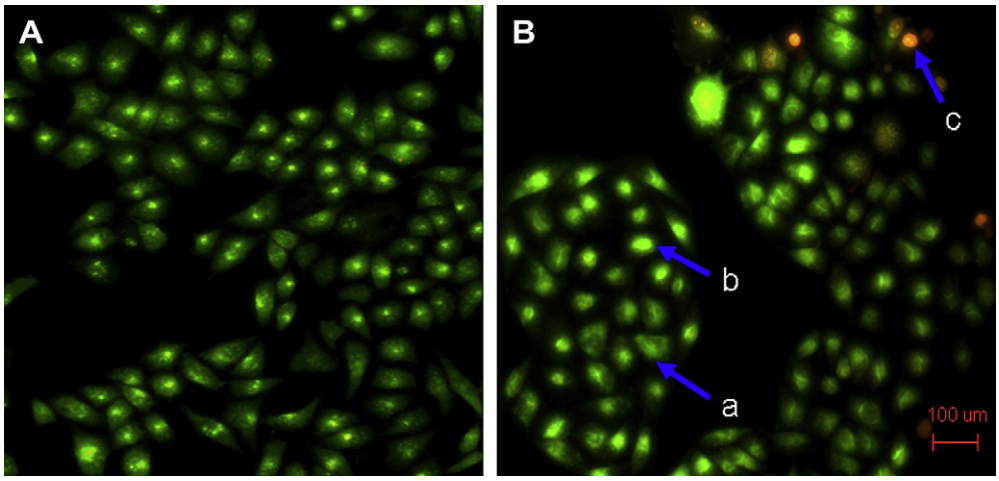

Fig. 8. BEL-7402 cell were stained by AO/EB and observed under fluorescence microscopy. BEL-7402 cell without treatment (a) and in the presence of complex **2** (b) incubated at 37 °C and 5% CO_2 for 24 h. Cells in a, b and c are living, apoptotic and necrotic cells, respectively.

3.11. Antioxidant activity against hydroxyl radical (•OH)

The hydroxyl radical (•OH) is one of the most reactive products of reactive oxygen species (ROS), which can result in cell membrane disintegration, membrane protein damage, DNA mutation and initiate the development of many diseases. In this report, the hydroxyl radical in aqueous media was generated by the Fenton system. The antioxidant activity of the ligands APIP, HAPIP and complexes **1** and **2** against hydroxyl radical (•OH) were investigated. As shown in Fig. 10 and Table 2, the inhibitory effect of the ligands and their Ru(II) complexes on •OH increased with increasing of the sample concentration in the range of 0.5–3.5 μM. The suppression ratio against •OH valued from 6.59 to 49.29 for APIP, 4.96 to 69.15 for HAPIP, 3.76 to 66.20 for complex **1** and 2.40 to 58.40 for complex **2**, respectively. The suppression ratio increased when APIP bonded Ru(II) metal center to form complex **1**, whereas the suppression ratio lessened for HAPIP to form complex **2** under the same experimental condition. The information obtained from the present work would

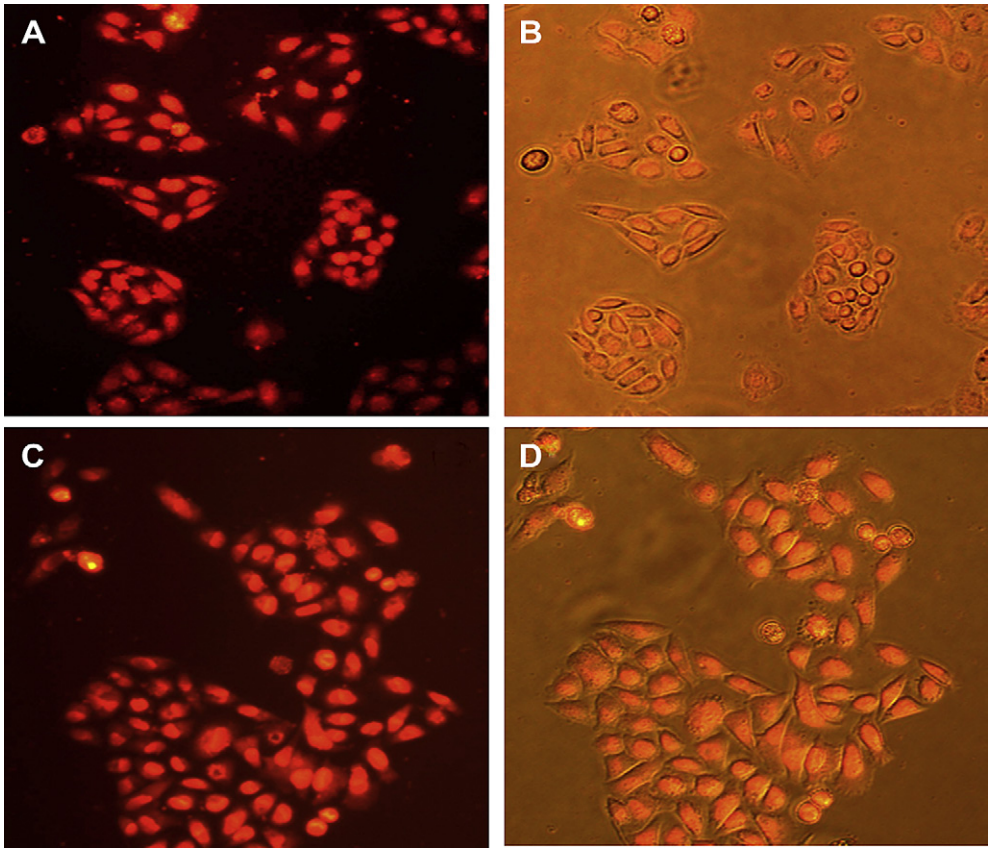

Fig. 9. BEL-7402 cells incubated with complexes **1** (25 μM, A and B) and **2** (50 μM, C and D) for 48 h imaged by fluorescence microscopy. A and C imaged under fluorescence, B and D imaged under fluorescence and visible light. Note that the cytoplasm is extensively stained with the Ru(II) complexes.

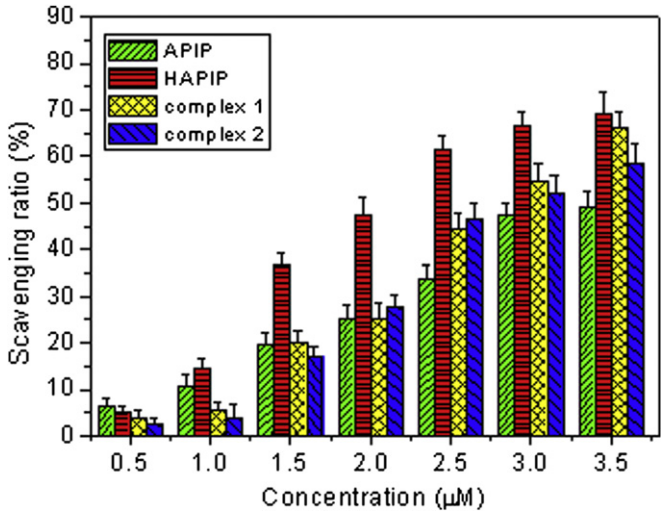

Fig. 10. Scavenging effect of the ligands and complexes on hydroxyl radicals. Experiments were performed in triplicate.

Table 2
The scavenging ratio (%) of ligands and complexes against •OH.

Compound	Average inhibition (%) for •OH						
	0.5	1.0	1.5	2.0	2.5	3.0	3.5
APIP	6.59	10.85	19.76	25.19	33.72	47.28	52.92
HAPIP	4.96	14.54	36.52	47.52	61.35	66.67	68.76
1	3.76	5.64	20.18	25.35	44.62	54.46	66.20
2	2.40	4.00	17.21	27.62	46.43	52.12	58.40

ultimately be helpful to develop new potential antioxidants and new therapeutic reagents for some diseases.

4. Conclusion

Two new ligands, APIP and HAPIP, and relative ruthenium(II) complexes $[Ru(phen)_2(APIP)](ClO_4)_2$ **1** and $[Ru(phen)_2(HAPIP)](ClO_4)_2$ **2** have been synthesized and characterized. The DNA-binding behaviors indicate that the two complexes can intercalate into DNA base pairs via intercalative ligands. When irradiated at 365 nm, complexes **1** and **2** can efficiently cleave the plasmid pBR 322 DNA. Cytotoxicity assay shows that complexes all display different antitumor activity against tumor cells tested. The apoptosis study indicates that complexes **1** and **2** can effectively induce apoptosis in BEL-7402 cells. The cellular uptake shows that complexes can enter into the cytoplasm and accumulate in the nuclei. The antioxidant activity experiments show that all these compounds possess high antioxidant activity.

Acknowledgments

This work was supported by the National Nature Science Foundation of China (Nos. 31070858, 30800227) and Guangdong Pharmaceutical University for financial supports.

References

[1] B. Norden, P. Lincoln, B. Akerman, E. Tuite, in: A. Sigel, H. Sigel (Eds.), Metal ions in biological systems, vol. 33, Marcel Dekker, New York, 1996, p. 177.
[2] K.E. Erkkila, D.T. Odom, J.K. Barton, Chem. Rev. 99 (1999) 2777–2796.
[3] C. Metcalfe, J.A. Thomas, Chem. Soc. Rev. 32 (2003) 215–224.
[4] L.H. Hurley, Natl. Rev. 2 (2002) 188–200.
[5] A.E. Friedman, J.C. Chambron, J.P. Sauvage, N.J. Turro, J.K. Barton, J. Am. Chem. Soc. 112 (1990) 4960–4962.
[6] F. Gao, H. Chao, F. Zhou, Y.X. Yuan, B. Peng, L.N. Ji, J. Inorg. Biochem. 100 (2006) 1487–1494.
[7] A.C.G. Hotze, S.E. Caspers, D. de Vos, H. Kooijman, A.L. Spek, A. Flamigni, M. Bacac, G. Sava, J.G. Haasnoot, J. Reedijk, J. Biol. Inorg. Chem. 9 (2004) 354–364.
[8] A.C.G. Hotze, B.M. Kariuki, M.J. Hannon, Angew. Chem. Int. Ed. 45 (2006) 4839–4842.
[9] C.G. Hartinger, S. Zorbas-Seifried, M.A. Jakupec, B. Kynast, H. Zorbas, B.K. Keppler, J. Inorg. Biochem. 100 (2006) 891–904.
[10] M. Galanski, V.B. Arion, M.A. Jakupee, B.K. Keppler, Curr. Pharm. Des. 9 (2003) 2078–2089.
[11] M.A. Fuertes, C. Alonso, J.M. Pérez, Chem. Rev. 103 (2003) 645–662.
[12] M.J. Clarke, F.C. Zhu, D.R. Frasca, Chem. Rev. 99 (1999) 2511–2534.
[13] U. Schatzschneider, J. Niesel, I. Ott, R. Gust, H. Alborzinia, S. Wölfl, Chem. Med. Chem. 3 (2008) 1104–1109.
[14] Y.J. Liu, C.H. Zeng, H.L. Huang, L.X. He, F.H. Wu, Eur. J. Med. Chem. 45 (2010) 564–571.
[15] S. Schäfer, I. Ott, R. Gust, W.S. Scheldrick, Eur. J. Inorg. Chem. 19 (2007) 3034–3046.
[16] H.L. Huang, Y.J. Liu, C.H. Zeng, L.X. He, F.H. Wu, DNA Cell Biol. 29 (2010) 261–270.
[17] J. Marmur, J. Mol. Biol. 3 (1961) 208–218.
[18] M.E. Reichmann, S.A. Rice, C.A. Thomas, P. Doty, J. Am. Chem. Soc. 76 (1954) 3047–3053.
[19] Y. Xiong, X.F. He, X.H. Zou, J.Z. Wu, X.M. Chen, L.N. Ji, R.H. Li, J.Y. Zhou, K.B. Yu, J. Chem. Soc. Dalton. Trans. 1 (1999) 19–24.
[20] J.G. Liu, B.H. Ye, H. Chao, Q.X. Zhen, L.N. Ji, Chem. Lett. 28 (1999) 1085–1086.
[21] B.P. Sullivan, D.J. Salmon, T.J. Meyer, Inorg. Chem. 17 (1978) 3334–3341.
[22] J.D. McGee, Biopolymers 15 (1976) 1345–1375.
[23] J.B. Chaires, N. Dattagupta, D.M. Crothers, Biochemistry 21 (1982) 3933–3940.
[24] S. Satyanaryana, J.C. Dabrowial, J.B. Chaires, Biochemistry 31 (1993) 9319–9324.
[25] G. Cohen, H. Eisenberg, Biopolymers 8 (1969) 45–55.
[26] T. Mosmann, J. Immunol. Methods 65 (1983) 55–63.
[27] D.L. Spector, R.D. Goldman, L.A. Leinwand, in: , In cells: A laboratory manual, vol. 1, Cold Spring Harbor Laboratory Press, New York, 1998 (Chapter 15).
[28] C.C. Winterbourn, Free Radic. Biol. Med. 3 (1987) 33–39.
[29] E.A. Steck, A.R. Day, J. Am. Chem. Soc. 65 (1943) 452–456.
[30] J.G. Liu, B.H. Ye, H. Li, Q.X. Zhen, L.N. Ji, Y.H. Fu, J. Inorg. Biochem. 76 (1999) 265–271.
[31] J.G. Liu, Q.L. Zhang, L.N. Ji, Y.Y. Cao, X.F. Shi, Transit. Met Chem. 26 (2001) 733–738.
[32] L.F. Tan, H. Chao, H. Li, Y.J. Liu, B. Sun, W. Wei, L.N. Ji, J. Inorg. Biochem. 99 (2005) 513–520.
[33] R.B. Nair, E.S. Teng, S.L. Kirkland, C.J. Murphy, Inorg. Chem. 37 (1998) 139–141.
[34] V. Rajendiran, M. Murali, E. Suresh, S. Sinha, K. Somasundaram, M. Palaniandavar, Dalton. Trans. 1 (2008) 148–163.
[35] S. Satyanarayana, J.C. Dabrowiak, J.B. Chaires, Biochemistry 32 (1993) 2573–2584.
[36] M.J. Waring, J. Mol. Biol. 13 (1965) 269–282.
[37] H.Q. Liu, B.C. Tzeng, Y.S. You, S.M. Peng, H.L. Chen, M.S. Yang, C.M. Che, Inorg. Chem. 41 (2002) 3161–3171.
[38] B. Elias, A.K.D. Mesmaeker, Coord. Chem. Rev. 250 (2006) 1627–1641.
[39] B. Armitage, Chem. Rev. 98 (1998) 1171–1200.
[40] J.K. Barton, A.L. Raphael, J. Am. Chem. Soc. 106 (1984) 2466–2468.
[41] H.L. Huang, G.P. Tang, Q.Q. Wang, D. Li, F.P. Shen, J. Zhou, H. Yu, Chem. Commun. (2006) 2382–2384.
[42] H.L. Huang, H. Yu, G.P. Tang, Q.Q. Wang, J. Li, Biomaterials 31 (2010) 1830–1838.
[43] B. Sun, J.X. Guan, L. Xu, B.L. Yu, L. Jiang, J.F. Kou, L. Wang, X.D. Ding, H. Chao, L.N. Ji, Inorg. Chem. 48 (2009) 4637–4639.
[44] L. Liu, H. Zhang, X.G. Meng, J. Yin, D.F. Li, C.L. Liu, Biomaterials 31 (2010) 1380–1391.